Engineering Structures 308 (2024) 117999

Contents lists available at ScienceDirect

Engineering Structures

journal homepage: www.elsevier.com/locate/engstruct

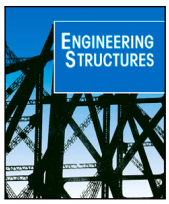

Estimation of pile stiffness in non-homogeneous soils through Artificial Neural Networks

Román Quevedo-Reina, Guillermo M. Álamo, Juan J. Aznárez *

Instituto Universitario de Sistemas Inteligentes y Aplicaciones Numéricas en Ingeniería, Universidad de Las Palmas de Gran Canaria, Edif. Central del Parque Científico-Tecnológico, Campus Universitario de Tafira, Las Palmas de Gran Canaria, 35017, Spain

ARTICLE INFO

Keywords:
Pile foundation
Soil–structure interaction
Non-homogeneous soils
Artificial Neural Network
Surrogate model

ABSTRACT

Many international standards highlight the relevance of studying the compatibility of forces and displacements between the structure and the foundation that supports it. In the case of pile foundations, some authors use continuum models that rigorously reproduce the interaction of the pile with the surrounding soil. However, their high computational cost justifies the use of simplified methodologies that allow obtaining sufficiently accurate results in significantly less time. This work presents a surrogate model based on Artificial Neural Networks (ANNs) trained from a synthetic dataset generated by a continuum numerical model. A good regression capacity is observed by the proposed model, also requiring very short evaluation times. Two use examples are presented to illustrate the smooth behaviour of the ANNs model and its ability to determine the critical pile length. This surrogate model allows introducing soil–structure interaction in problems with large volume of evaluations in a feasible way without significantly compromising the confidence of the results.

1. Introduction

Knowing the foundation behaviour and the effects that it can induce on the structure is a fundamental task for a correct structural analysis. For this reason, many standards highlight the relevance of determining the deformations produced in the foundation, as well as the compatibility with the forces and movements of the structure it supports (see, e.g., [1–3]).

Without being exhaustive, there are two well-known methodologies in the literature that allow obtaining the stiffness of pile foundations. Models based on Winkler-type methodologies are the most popular, where the soil–pile interaction is treated as a set of independent distributed springs for which there are proposals for their stiffness value to obtain accurate solutions to many problems. These models can have a simple mathematical formulation that allows access to numerical or analytical solutions that are very useful in the early stages of design. The American Petroleum Institute (API) proposes using this model [2], which allows introducing non-linearities in the springs that modify soil response depending on the lateral displacement of the pile at different depths ("p-y" formulations). Another approach is directly using numerical models that allow studying the continuum problem including the pile foundation and the soil. This methodology, mainly based on the Finite Element Method or the Boundary Element Method, rigorously considers the interaction of the pile with the surrounding soil with greater naturalness and precision depending on the method employed. In this way, the three-dimensional nature of this interaction is taken into account where the soil is considered as an infinite medium constituted by layers with different properties that extends beyond the pile in all directions. An actualized review of this topic can be consulted in [4]. Also, with some of these methodologies, several authors have proposed explicit expressions of the stiffness for a pile foundation (see, e.g., [5–12]). These formulas allow a very fast and simple evaluation, although they have been obtained for specific soil profiles and therefore do not allow to collect more complex behaviours of the soil–structure interaction.

In contrast to these numerical models, the use of Machine Learning (ML) techniques with the aim of developing general surrogate models (meta-modelling) can be a simple, accessible and useful option to capture the complex phenomena involved in this problem. The interest in these tools has increased within the field of civil engineering in recent years [13,14]. More specifically, the application of different artificial intelligence (AI) techniques in geotechnical engineering has achieved satisfactory results for many problems of interest [15]. This review also highlights Artificial Neural Networks (ANNs) as the predominant tool among all those analysed. In this sense, a recent review that is much more focused on the application of ANN tools in this type of problems can be found in Moayedi et al. [16]. Furthermore, Shanin [17] and Fatehnia et al. [18] provide some interesting and extensive reviews

* Corresponding author.
E-mail address: juanjose.aznarez@ulpgc.es (J.J. Aznárez).

https://doi.org/10.1016/j.engstruct.2024.117999
Received 13 January 2024; Received in revised form 29 March 2024; Accepted 8 April 2024
Available online 16 April 2024

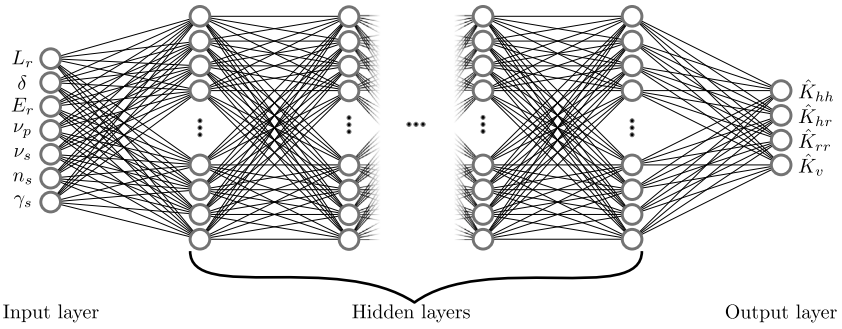

Fig. 1. Conceptual diagram of the fully connected neural network using in this work, highlighting the input layer, the hidden layers and the output layer. Input and output variables included are properly defined in Section 3.

on the implementation of AI techniques, including ANN, in pile foundation design and analysis. The application of such techniques in the development of surrogate models to evaluate the stiffness of pile foundations is a necessary and undeveloped task. To the best of the authors' knowledge, only a study of Franza et al. [19] has been found, where an ANN has been trained to evaluate the impedance functions of 2x2 inclined pile groups in homogeneous soils. At the present time these metamodels can be formulated with guarantees, accuracy, and generality and are a very interesting alternative to incorporate with economy and simplicity the soil–structure interaction effects in other structural models.

Thus, the aim of this article is to develop a Artificial Neural Network based model (ANN-based model) capable of reproducing the equivalent linear stiffness of a pile foundation in non-homogeneous soil according to a continuum model. This is an initial approach to the implementation of Machine Learning techniques to the study of the compatibility of forces and movements between these deep foundations and the structure they support.

2. Methodology

2.1. ANN-based model

The ANN-based model capable of estimating the stiffness of the pile is built through a supervised learning process, that requires a dataset with example cases from which the neural network can learn. Due to the difficulty of obtaining a sufficiently large volume of experimental data, a synthetic dataset is built from an available numerical model (see Section 2.2). For the generation of this dataset, the limits of the search space of the input variables must be defined. Next, using uniformly distributed random numbers, random cases are generated between the established limits, obtaining the input variables of the dataset. Finally, the continuum model, which is intended to be replaced by the neural network, is used to evaluate the dataset inputs and thus obtain the outputs.

Since the problem to solve corresponds to a regression problem with unstructured data (there is no spatial or sequential structure), it is proposed to use fully connected networks (represented in Fig. 1). In this case, the number of parameters that the network will present, as well as its capacity to fit the data, will closely depend on the number of hidden layers and the number of neurons per layer. For this work, different architectures will be analysed by modifying the number of hidden layers and neurons per layer. To reduce architecture variability, all hidden layers are assumed to have the same number of neurons. In addition, at the output of each hidden layer, a normalization of the layer is performed to speed up its training [20] and the Rectified Linear Unit ($\mathrm{ReLU}(x) = \max(0, x)$) is used as activation function.

To reduce the differences in scale of the different input and output variables, they are normalized by subtracting the mean and dividing by the standard deviation. Next, the dataset is randomly divided into two parts: a training dataset (80%) by which the error is minimized, and a validation dataset (20%) to stop the training and avoid overfitting.

The training of the neural network is carried out using the automatic differentiation algorithm already implemented in Matlab [21], and setting the mean squared error ($\mathrm{MSE} = \frac{1}{n}\sum_{i=1}^{n}(\hat{Y} - Y)^2$) of the outputs as the loss function. For updating the parameters, the adaptive moment estimation [22] is used with an initial global learning rate of 0.01, a gradient decay factor of 0.9, a squared gradient decay factor of 0.999 and a batch size of 5000. The error of the validation data is continuously evaluated, stopping the training when it stabilizes. Next, the neural network is retrained, reducing the global learning rate by half, repeating this process until the new network does not improve the results of the previous one.

Finally, once the training and evaluation of the ANNs have been carried out, it is proposed to combine the predictions of independent networks to build an ensemble model (see, e.g., [23]). In this way, the output of the ensemble model would be defined as the mean of the predictions of the individual networks, so large local errors of some networks can be reduced by the agreement of others. In addition, a measure of prediction uncertainty can be obtained by evaluating the standard deviation of the individual ANNs outputs.

2.2. Continuum model for computing the pile stiffness

The dataset is an essential element for the supervised learning process. In this work, a synthetic dataset is generated using an previously developed rigorous continuum numerical model [24] that has been verified and successfully employed in the analysis of several soil–structure interaction problems (see, e.g., [25,26]). This model is based on the integral expression of the reciprocity theorem in elastodynamics and the use of advanced fundamental solutions for reproducing the behaviour of the layered soil. These fundamental solutions already satisfy the free-field and inter-layer boundary conditions, which avoid any meshing of the soil surfaces. On the other hand, piles are treated as load lines in the soil formulation and their stiffness and inertial contribution are considered through their definition as finite elements beams. Pile-soil coupling is made by imposing compatibility and equilibrium conditions in terms of displacements and soil–pile interaction forces, respectively. Linear-elastic behaviour of soil and piles is considered. Despite it is a model generally oriented to the analysis of dynamic problems in the frequency domain, it is implemented in such a way that it can reproduce the corresponding static problem assuming sufficiently low frequency. In this study, results are obtained considering a wavelength of the shear wave of the soil at reference depth 100 times greater than the pile diameter. These assumptions result in a very efficient but accurate model.

The numerical model used is formulated for layered soils. In order to reproduce a continuous variability of soil properties, the soil profile is discretized into enough layers of constant properties, achieving an equivalent global behaviour.

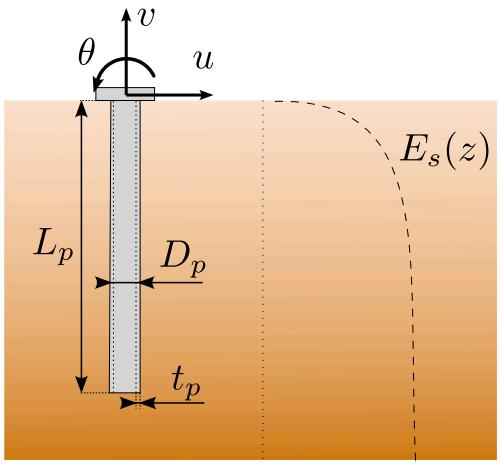

Fig. 2. Problem statement. Single hollow pile embedded in non-homogenous halfspace.

As aforementioned, this numerical model presents some simplifications. Linear elastic behaviour is considered both for pile and soil; and the contact between them is assumed to be perfectly welded. The pile is treated as a beam element, reducing its dimension to its axis and, therefore, not affecting the soil continuity. However, the authors [25] have demonstrated its applicability, even for significantly non-slender foundations, through a comparison against a soil-shell interaction model.

3. Problem statement

This work aims to characterize the static stiffness of pile foundations in non-homogeneous soils, such as the one represented in Fig. 2. The pile is considered as a tubular element embedded in a vertical position. The geometric variables that define it are the embedded length (L_p), the diameter (D_p) and the thickness (t_p). For the static analysis, the material characteristics are reduced to Young's modulus (E_p) and Poisson's ratio (ν_p). The soil is considered as a non-homogeneous vertical halfspace with mechanical properties defined by a shear wave velocity that increases continuously with depth following a generalized power law function [27]. As this work focuses on the static stiffness of foundations, this power law is rewritten in terms of Young's modulus as:

$$E_s(z) = E_s^L \left(b + (1-b)\,\frac{z}{L_p} \right)^{2n_s} \quad \text{with} \quad b = \left(\frac{E_s^0}{E_s^L} \right)^{\frac{1}{2n_s}} \tag{1}$$

where L_p is the pile length (used as reference depth), E_s^0 and E_s^L are the Young's modulus at the free surface and at the reference depth, respectively, and n_s is a dimensionless parameter that determine the Young's modulus profile between the free surface and the reference depth.

The stiffness of the pile is associated with three degrees of freedom: lateral displacement (u), rotation (θ) and vertical displacement (v) of the head (Fig. 2). Due to the radial symmetry that the problem presents, it is redundant to determine what happens to the lateral displacement and the rotation in the perpendicular plane. In this way, the pile stiffness matrix presents the following structure:

$$\begin{Bmatrix} F_u \\ F_\theta \\ F_v \end{Bmatrix} = \begin{bmatrix} K_{hh} & K_{hr} & 0 \\ K_{hr} & K_{rr} & 0 \\ 0 & 0 & K_v \end{bmatrix} \begin{Bmatrix} u \\ \theta \\ v \end{Bmatrix} \tag{2}$$

where K_{hh} is the horizontal stiffness (lateral force on pile head due to an unitary lateral displacement), K_{rr} is the rocking stiffness (bending moment on pile head due to an unitary rotation), K_{hr} is the horizontal-rocking coupling stiffness (bending moment on pile head due to an unitary lateral displacement and lateral force on pile head due to an unitary rotation), and K_v is the vertical stiffness (vertical force due to an unitary vertical displacement).

Table 1
Limits established for the dimensionless variables that define the problem.

Variable	Lower limit	Upper limit
L_r	0	100
δ	0	1
E_r	10	$5 \cdot 10^4$
ν_p	0.15	0.35
ν_s	0.15	0.5
n_s	0	1
γ_s	0	1

Once the system has been defined, applying Buckingham's theorem [28], the problem is dimensionless treated in order to reduce the number of variables. The dimensionless variables used to define the system under study are:

$$L_r = \frac{L_p}{D_p} \qquad E_r = \frac{E_p}{E_s^L}\left(1-\delta^4\right) \qquad \nu_s \qquad \gamma_s = \sqrt{\frac{E_s^0}{E_s^L}}$$
$$\delta = 1 - \frac{2\,t_p}{D_p} \qquad \nu_p \qquad n_s \tag{3}$$

while the dimensionless stiffness are:

$$\hat{K}_{hh} = \frac{K_{hh}}{E_s^L\,D_p} \qquad \hat{K}_{hr} = \frac{K_{hr}}{E_s^L\,D_p^2}$$
$$\hat{K}_{rr} = \frac{K_{rr}}{E_s^L\,D_p^3} \qquad \hat{K}_v = \frac{K_v}{E_s^L\,D_p} \tag{4}$$

To focus the study within a coherent scenario according to the possible systems, a series of lower and upper limits are established for each of the dimensionless variables that define the problem. These limits are shown in Table 1.

Note that the reliability of the surrogate model predictions is limited to those regions within the search space, decreasing closer to the boundaries. However, a large number of scenarios is covered by this search space. The considered soil profile is a halfspace with a general power-law stiffness variability trough depth. The n_s and γ_s parameters allow reproducing different variations of the properties with depth, including the homogeneous halfspace as a particular case. Regarding to the pile geometry, from solid to thin-walled hollow piles are including, with very wide slenderness ratios. The Young's modulus of the soil can range from 4.2 MPa, if a solid steel pile is assumed ($E_p = 210$ GPa), up to 2.7 GPa if the pile is made of concrete ($E_p = 27$ GPa). With respect to the Poisson's ratio, in the case of the pile the search space includes the characteristic values of concrete ($\nu_p = 0.2$) and steel ($\nu_p = 0.3$), while for the soil it is extended to include saturated soils ($\nu_s \approx 0.5$).

4. Results

4.1. Architecture selection

As indicated in Section 2.1, in order to generate the ANNs based model, a dataset for training the model is needed (which will be divided into the training dataset and the validation dataset), which in this case has 200,000 cases. In addition, for the required evaluation of the models, a test dataset of 150,000 cases is also generated. In a balance between computational cost and performance, a small study is performed to achieve sufficient predictive capacity in the resulting model while avoiding training an excessive number of oversized ANNs. To analyse the architecture relevance, 20 different architectures are defined. The number of hidden layers and the neurons per hidden layer is randomly selected within the intervals from 2 to 5 and from 50 to 200, respectively. Table 2 shows the number of hidden layers and the number of neurons per hidden layer of the generated architectures.

Table 2
Definition of architectures used.

Id.	1	2	3	4	5	6	7	8	9	10
No. of hidden layers	2	2	2	2	3	4	3	2	3	3
No. of neurons per hidden layer	50	65	70	80	60	50	70	110	90	100
No. of parameters	3354	5334	6094	7764	8404	8654	11,204	13,974	18,004	22,004
Id.	11	12	13	14	15	16	17	18	19	20
No. of hidden layers	3	5	5	2	4	2	3	3	4	5
No. of neurons per hidden layer	110	80	90	180	105	195	145	170	165	145
No. of parameters	26,404	27,684	34,744	35,464	35,494	41,344	44,954	61,204	85,474	87,874

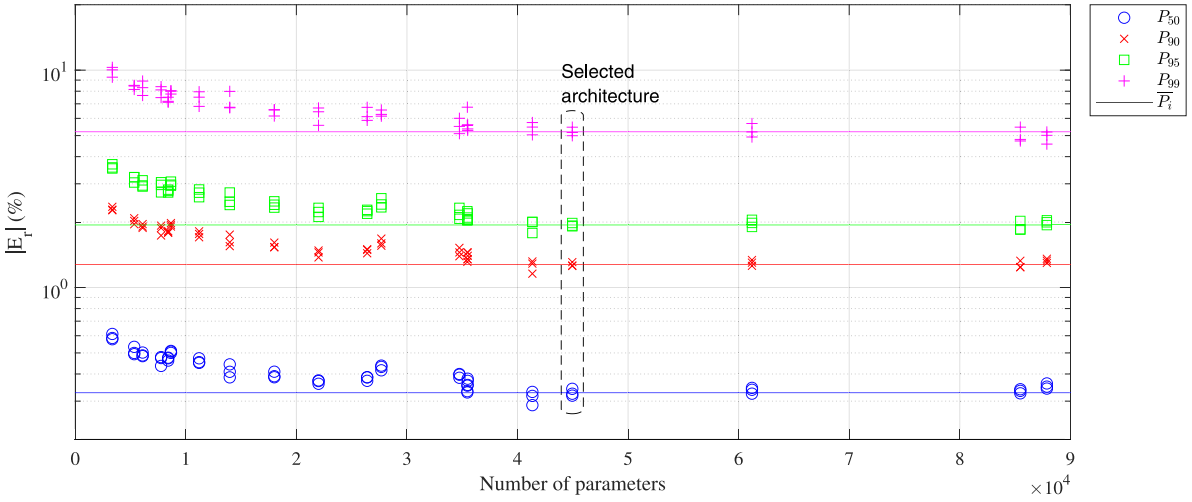

Fig. 3. The 50th, 90th, 95th and 99th percentiles of the relative errors obtained by trained neural networks evaluated over test dataset.

For each of the established architectures, 3 repetitions are performed in order to reduce the statistical fluctuations due to the stochastic processes associated with these models.

Once the training of the 60 neural networks described has been completed, the aim is to compare their performance. To do this, the test dataset is evaluated and the relative error in absolute value of the prediction $(\hat{Y})$ related to the value of the continuum numerical model (Y) is obtained:

$$|E_r|(\%) = 100 \cdot \left| \frac{\hat{Y} - Y}{Y} \right| \tag{5}$$

The 50th, 90th, 95th and 99th percentiles of error distributions are selected as measures of the performance of the neural network. Fig. 3 shows the results for the different architectures used, where the different markers represent the value of the 50th, 90th, 95th and 99th percentiles obtained for the ANNs trained. As expected, the error in the predictions decrease while the number of parameters increases, stabilizing over 40,000 parameters. Based on this trend, it is not necessary to increase the range of the architecture study. According to the results, the architecture with 3 hidden layers and 145 neurons per hidden layers is established for the pretended model, being their results surrounded by a dashed line in Fig. 3. Also, to help the comparison, solid lines are used to mark the mean value among the three repetitions of each percentile of the selected architecture.

4.2. Performance of ANN model

After defining the architecture of the neural network that will be used in the proposed model, 17 networks of the same topology are additionally trained to obtain a total of 20 independent ANNs. In this way, the prediction of each of them can be combined to obtain an ensemble model that consists of the mean value of each individual network. To evaluate the performance of the different networks and the ensemble model, the test dataset is evaluated and the relative error in absolute value of each measurement is obtained (Eq. (5)). Fig. 4 represents the complementary cumulative distribution function of the error of the four stiffness terms of each one of the 20 networks individually evaluated and of the ensemble model built from them. It is observed that, from a statistical point of view, the ensemble model significantly improves the performance of individual networks. In a more detailed comparison, individual networks present an average error greater than 3.7% in the horizontal stiffness for only 1% of the cases, while the ensemble model presents an error greater than 2.4% for 1% of the cases. Similarly, this reference error is reduced from 4.6% to 2.3% for horizontal-rocking coupling stiffness, from 9% to 3.6% for the rocking stiffness and from 4.2% to 2.5% for vertical stiffness.

Fig. 5 groups the complementary cumulative distribution function of the error of the ensemble model for the four stiffness estimated in order to be easily compared. It should be noted that the errors do not present a homogeneous distribution among them, where horizontal stiffness and rocking stiffness stand out. The former presents higher relative errors for a large percentage of samples, while the deviations it presents are smaller than for the other stiffness terms for the worst predicted cases. On the other hand, for rocking stiffness, the opposite occurs. In any case, this fact does not affect the global performance of the model, since only a 10% error in the prediction is exceeded in the 0.3% of the rocking stiffness, the 0.13% of the cross stiffness and the vertical stiffness, and the 0.07% of the horizontal stiffness. It should be mentioned that there are some cases for which errors of up to 100% are obtained, although with a very low prevalence (less than 0.013% in the most frequent case). However, the difference in computation times justifies using this surrogate model: the average execution time of the continuous model is around 61.25 s, while in the ensemble model it is around $1.04 \cdot 10^{-4}$ s, both executions performed parallelized in a 40-core (Intel® Xeon® Gold 6242R CPU @ 3.10 GHz), 93 GB RAM computer.

Other advantage of the ensemble model is that it provides a measure of prediction uncertainty through the standard deviation of the results given by each individual net. The relationship between the prediction

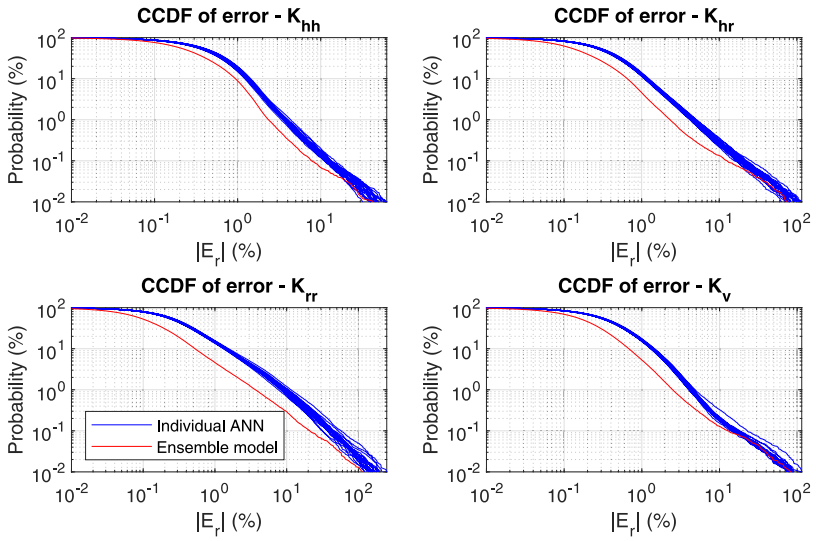

Fig. 4. Complementary cumulative distribution function (CCDF) of the error in the predictions for the individuals ANNs and the ensemble model.

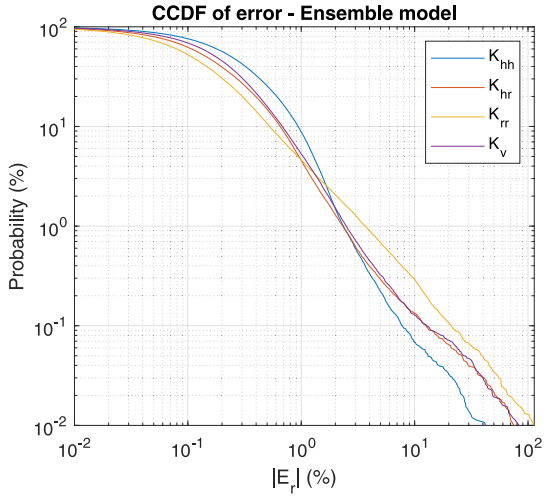

Fig. 5. Complementary cumulative distribution function (CCDF) of the error in the predictions for the ensemble model.

dispersion and the error of the surrogate model is analysed in Fig. 6. This figure shows a heatmap of the number of observations of the relative error, in absolute value, and the coefficient of variation obtained from the ensemble model ($|CV|$). The coefficient of variation is defined as the absolute value of the standard deviation of the individual predictions of each net divided by their mean value. A significant relationship between the relative error and the coefficient of variation is observed. The diagonal dashed line marks the points where both metrics coincide. Furthermore, those cases whose error is considerable larger than the model uncertainty (i.e., points above the diagonal dashed line) correspond to small relative errors, not compromising the reliability of the surrogate model. Note that the horizontal dotted line marks the limit of a relative error equal to 1%.

4.3. Application examples

To show the ability of the proposed surrogate model to reproduce the behaviour of single pile foundations in terms of its head stiffness, two application examples are presented.

First, in Fig. 7, the results of the ensemble model are compared with well-established fitted expressions [8–12] for the lateral, rocking and cross-coupled stiffness of a flexible pile embedded in homogeneous soils or soils with a linearly varying stiffness profile. These expressions, which define the head stiffness as a function of the pile-soil relative stiffness, can be consulted in the original works or in the recent review made by Mylonakis and Crispin [4]. In all this works, the soil with a linear variation of its Young's modulus has zero stiffness at surface level ($\gamma_s = 0$, $n_s = 0.5$). The results of the ensemble model are obtained assuming $L/D = 50$, $\delta = 1$ (solid cross-section), $\nu_p = 0.25$, and $\nu_s = 0.5$ (as in [12]).

The comparison presented in Fig. 7 shows a nice agreement between the results computed by the ensemble model and those obtained by the different fitted expressions. Furthermore, the surrogate model is capable to smoothly reproduce the influence of the pile-soil relative stiffness on the three stiffness terms without noise or discontinuities. Discrepancies between the ensemble model and formulas are higher for the lateral stiffness, while for the rocking term almost all approaches converge into the same values. The same level of good agreement is found both for the homogeneous and non-homogeneous profiles.

For the second application example, the dimensional problem of computing the pile head stiffness of a large-sized hollow monopile is handled. These foundations are typically used as the supporting structures for offshore wind turbines. The influence of both the pile length and soil profile on the four pile stiffness terms is analysed. For that purpose, three variable-with-depth soils ($n_s = 0.2, 0.5$ and 0.8) and one homogeneous soil ($n_s = 0$) are considered. All profiles presents the same average stiffness over their first 30 m, $\bar{E}_{s,30} = 30$ MPa, and a constant Poisson ratio $\nu_s = 0.49$ (equivalent to a saturated soil). For the non-homogeneous media, a zero stiffness at surface level is assumed ($\gamma_s = 0$). The evolution with depth of the Youngs modulus with respect to the average value is presented for the studied profiles in the right graphic area of Fig. 8. The pile geometry is defined by the dimensional properties: $D_p = 5$ m, $t_p = 57$ mm (following API's recommendation [2]), $L_p = 5$–40 m. Steel material properties are assumed for the pile: $E_p = 210$ GPa, $\nu_p = 0.25$.

Fig. 8 presents the four pile head stiffness terms as functions of the pile length. The results of the ensemble model for each soil profile are shown by different line colours, while crosses are used to represent the reference values obtained with the numerical model. A great agreement is observed between the predictions made by the ensemble model and the numerical model, even in this example where a significantly flexible pile (close to the lower limit presented in Table 1) is considered. As in the previous example, the pile stiffness computed by the surrogate model present a smooth behaviour with the variation of the pile length. The convergence into a fixed stiffness when the pile active length is

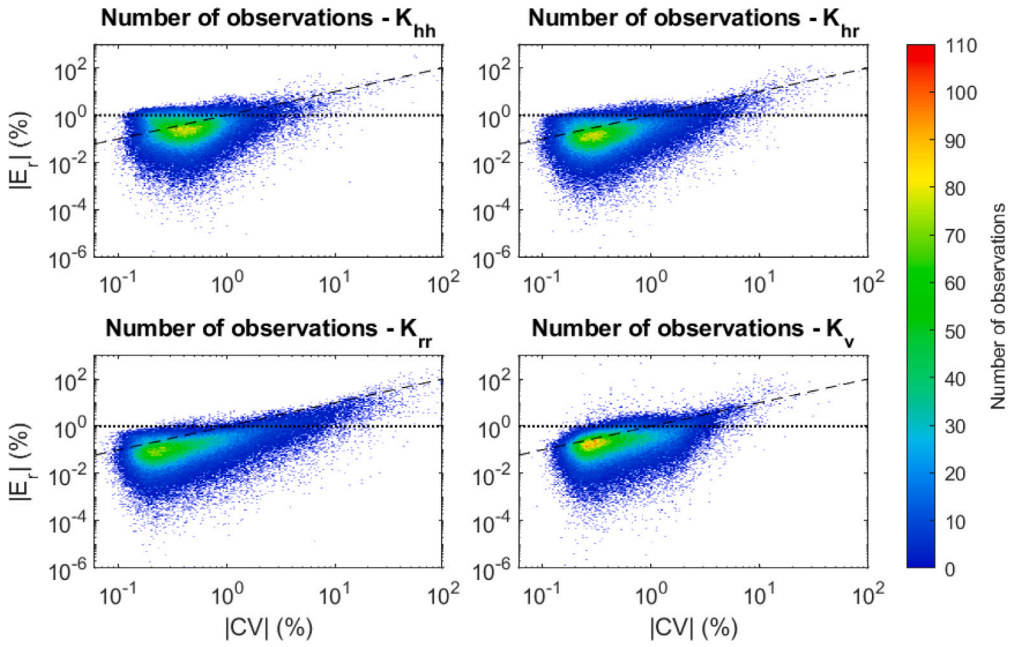

Fig. 6. Heatmap of the number of observations of the relative error and the coefficient of variation of the surrogate model.

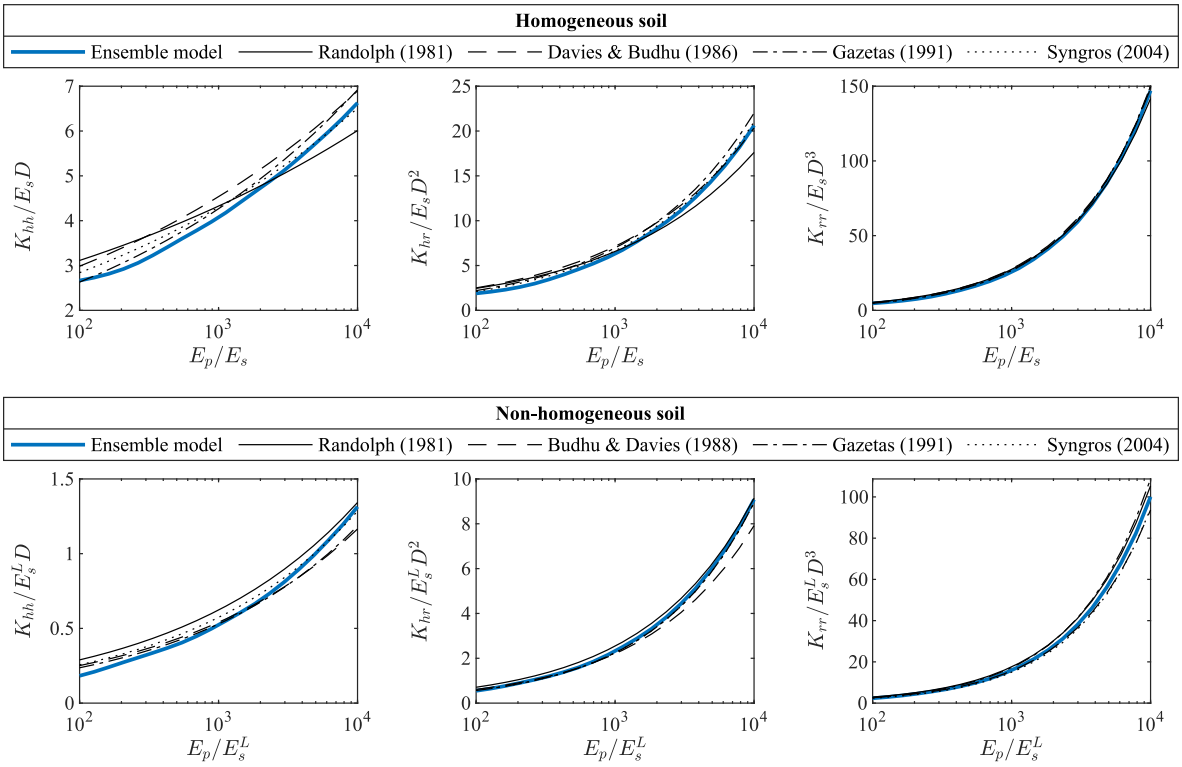

Fig. 7. Pile head stiffness for the lateral behaviour of a single pile depending on the pile-soil relative stiffness. Comparison of the ensemble model against fitted expressions.

reached is clearly seen for the terms related to the lateral behaviour (lateral, rocking and cross-swaying stiffness). Furthermore, the results show that the active length increases as the soil profile becomes softer near the free-surface, i.e, n_s increases. This trend qualitative agrees with the expressions presented in [29]. The expected relation between pile stiffness and length is obtained: as the pile grows longer, it reaches stiffer soils which leads to an increment of the foundation stiffness. However, as the impact of deeper soil layers is not the same for all terms [30,31], different behaviours are obtained. The horizontal stiffness, which is mainly influenced by the superficial soil properties, presents its maximum value for the homogeneous medium, and reduces its values as the soil becomes softer. The same trend is observed in the rocking and horizontal-rocking coupling terms for short piles. However, when the pile is long enough, the additional resistance of the deeper layers against the pile deflection reduce the difference of the rocking and coupled stiffness with respect to the homogeneous profile. The value of the active length for the rocking problem is larger than the one corresponding to the lateral problem. The extreme scenario is found

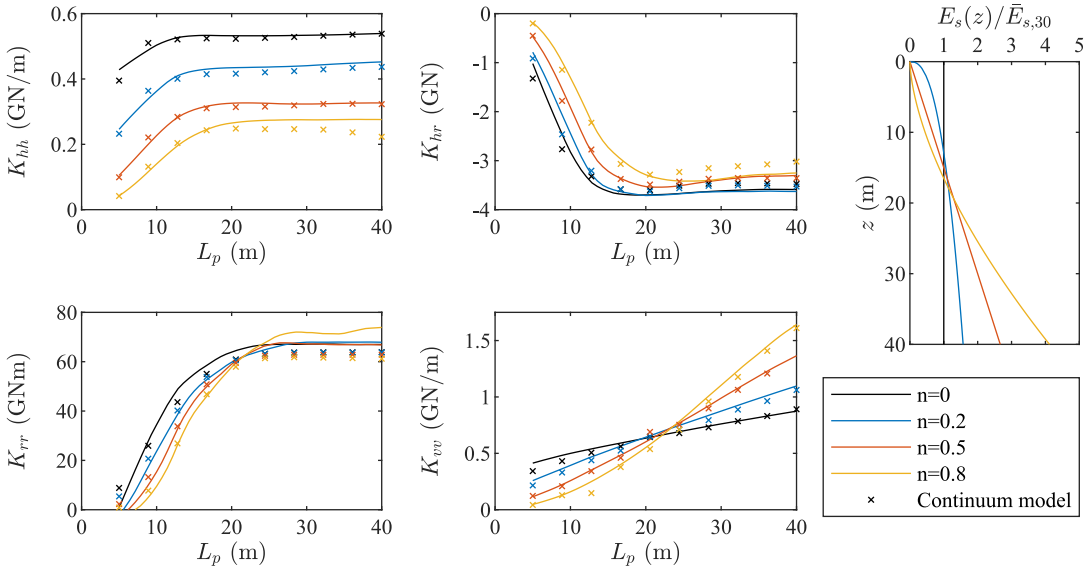

Fig. 8. Influence of pile length on the head stiffness for large diameter monopiles embedded in several soil profiles with the same average stiffness. Results comparing the ensemble model and the continuum model.

for the vertical stiffness, which is affected by soil properties along the whole pile. Thus, the vertical stiffness constantly increases with the pile length. The ratio of this increment is proportional to the ratio of the increment of the soil Young's modulus with depth.

5. Conclusions

A surrogate model based on ANNs which allow to reproduce the pile foundation stiffness is presented. The combined use of individuals neural networks in an ensemble model allows to increase the prediction capacity of it. The ensemble model reaches a high performance, obtaining relative errors less than 10% for 99.7%, 99.87% and 99.93% of the validation samples for the rocking stiffness, cross and vertical stiffness, and lateral stiffness terms, respectively. This performance is achieved with a significant reduction in the computational cost, allowing the evaluation of a thousand cases in less than one second.

Two application examples are included to illustrate the performance of the surrogate model with specific cases. First, the output of the model is compared with limited-range expressions present in the bibliography, showing a great agreement with them. In the second example, the evolution of the pile stiffness as its length increases is studied, while comparing the results of the surrogate model and the continuous model. A great agreement is shown between both models. The stabilization of the pile stiffness derived of reaching the active length is adequately reproduced by the surrogate model, allowing to determine this critical aspect of the foundation. In both examples, the surrogate model presents a smooth behaviour, which makes it a useful tool to propose previous parametric studies or perform fast estimations in first stages of studies that require the evaluation of a large volume of cases.

This work confirmed the capability of ANNs-based surrogate models for predicting the static response of pile foundations. As future works, different relevant phenomena, such as the dynamic response of the system and pile-soil–pile interaction, could be incorporated.

CRediT authorship contribution statement

Román Quevedo-Reina: Conceptualization, Formal analysis, Investigation, Methodology, Software, Validation, Visualization, Writing – original draft, Writing – review & editing. **Guillermo M. Álamo:** Conceptualization, Methodology, Supervision, Visualization, Writing – original draft, Writing – review & editing. **Juan J. Aznárez:** Conceptualization, Funding acquisition, Project administration, Writing – review & editing.

Declaration of competing interest

The authors declare that they have no known competing financial interests or personal relationships that could have appeared to influence the work reported in this paper.

Data availability

Data will be made available on request.

Acknowledgements

This study was supported by the Ministerio de Ciencia e Innovación and the Agencia Estatal de Investigación of Spain (MCIN/AEI/10.13039/501100011033) through Research Project PID2020-120102RB-I00 and FPU research fellowship FPU19/04170 from the Ministerio de Universidades (MIU) of Spain (Román Quevedo-Reina). In addition, it has also been partially supported by Agencia Canaria de Investigación, Innovación *y* Sociedad de la Información (ACIISI), Spain-Gobierno de Canarias and European ERDF Funds Grant EIS 202104. Finally, the authors would like to thank Samuel González Jiménez (Programa INVESTIGO ULPGC 32/39/2022-0923131539 from Servicio Canario de Empleo, Funds of The Recovery, Transformation and Resilience Plan Next Generation EU) for his collaboration in the adaptation of the supplementary material.

Appendix A. Supplementary data

Supplementary material related to this article can be found online at https://doi.org/10.1016/j.engstruct.2024.117999.

The developed surrogate model is available for download as a Matlab code or app from the research group's website (http://www.mmc.siani.es/software/).

References

[1] European Committee for Standardization. EN 1997-1 Eurocode 7: Geotechnical design - Part 1: General rules. CEN; 2005.
[2] American Petroleum Institute. API RP 2A-WSD: Recommended Practice for Planning , Designing and Constructing Fixed Offshore Platforms-Working Stress Design. 2007, Api recommended practice, 24-WSD.
[3] DNV GL AS. DNVGL-RP-C212: Offshore soil mechanics and geotechnical engineering. 2017, DNV GL - recommended practice, August.

[4] Mylonakis GE, Crispin JJ. Simplified models for lateral static and dynamic analysis of pile foundations. In: Analysis of pile foundations subject to static and dynamic loading. CRC Press; 2021, p. 185–245. http://dx.doi.org/10.1201/9780429354281-6.
[5] Poulos HG, Davis EH. Pile foundation analysis and design. Wiley New York; 1980, x, 397.
[6] Gazetas G. Seismic response of end-bearing single piles. Int J Soil Dyn Earthq Eng 1984;3(2):82–93. http://dx.doi.org/10.1016/0261-7277(84)90003-2.
[7] Pender MJ. Aseismic pile foundation design analysis. Bull New Zealand Natl Soc Earthq Eng 1993;26:49–160. http://dx.doi.org/10.5459/bnzsee.26.1.49-160.
[8] Randolph MF. The response of flexible piles to lateral loading. Géotechnique 1981;31(2):247–59. http://dx.doi.org/10.1680/geot.1981.31.2.247.
[9] Davies TG, Budhu M. Non-linear analysis of laterally loaded piles in heavily overconsolidated clays. Géotechnique 1986;36(4):527–38. http://dx.doi.org/10.1680/geot.1986.36.4.527.
[10] Budhu M, Davies TG. Analysis of laterally loaded piles in soft clays. J Geotech Eng 1988;114(1):21–39. http://dx.doi.org/10.1061/(ASCE)0733-9410(1988)114:1(21).
[11] Gazetas G. Formulas and charts for impedances of surface and embedded foundations. J Geotech Eng 1991;117(9):1363–81. http://dx.doi.org/10.1061/(ASCE)0733-9410(1991)117:9(1363).
[12] Syngros K. Seismic response of piles and pile-supported bridge piers evaluated through case histories [Ph.D. thesis], New York, USA: The City College of the City University of New York; 2004.
[13] Salehi H, Burgueño R. Emerging artificial intelligence methods in structural engineering. Eng Struct 2018;171:170–89. http://dx.doi.org/10.1016/j.engstruct.2018.05.084.
[14] Falcone R, Lima C, Martinelli E. Soft computing techniques in structural and earthquake engineering: A literature review. Eng Struct 2020;207. http://dx.doi.org/10.1016/j.engstruct.2020.110269.
[15] Baghbani A, Choudhury T, Costa S, Reiner J. Application of artificial intelligence in geotechnical engineering: A state-of-the-art review. Earth-Sci Rev 2022;228:103991. http://dx.doi.org/10.1016/j.earscirev.2022.103991.
[16] Moayedi H, Mosallanezhad M, Rashid ASA, Jusoh WAW, Muazu MA. A systematic review and meta-analysis of artificial neural network application in geotechnical engineering: Theory and applications. Neural Comput Appl 2020;32(2):495–518. http://dx.doi.org/10.1007/s00521-019-04109-9.
[17] Shahin MA. State-of-the-art review of some artificial intelligence applications in pile foundations. Geosci Front 2016;7(1):33–44. http://dx.doi.org/10.1016/j.gsf.2014.10.002.
[18] Fatehnia M, Amirinia G. A review of genetic programming and artificial neural network applications in pile foundations. Int J Geo-Eng 2018;9(1). http://dx.doi.org/10.1186/s40703-017-0067-6.
[19] Franza A, DeJong M, Morici M, Carbonari S, Dezi F. Artificial neural networks for the evaluation of impedance functions of inclined pile groups. In: Numerical Methods in Geotechnical Engineering IX: Proceedings of the 9th European Conference on Numerical Methods in Geotechnical Engineering. NUMGE 2018, 2018.
[20] Ba JL, Kiros JR, Hinton GE. Layer Normalization. 2016, http://dx.doi.org/10.48550/ARXIV.1607.06450.
[21] Matlab, deep learning toolbox, version 9.9.0.1592791 (r2020b) update 5. Natick, Massachusetts: The MathWorks Inc.; 2020.
[22] Kingma DP, Ba J. Adam: A method for stochastic optimization. 2014, http://dx.doi.org/10.48550/ARXIV.1412.6980, URL https://arxiv.org/abs/1412.6980.
[23] Folino G, Sabatino P. Ensemble based collaborative and distributed intrusion detection systems: A survey. J Netw Comput Appl 2016;66:1–16. http://dx.doi.org/10.1016/j.jnca.2016.03.011.
[24] Álamo GM, Martínez-Castro AE, Padrón LA, Aznárez JJ, Gallego R, Maeso O. Efficient numerical model for the computation of impedance functions of inclined pile groups in layered soils. Eng Struct 2016;126:379–90. http://dx.doi.org/10.1016/j.engstruct.2016.07.047.
[25] Álamo GM, Bordón JDR, Aznárez JJ. On the application of the beam model for linear dynamic analysis of pile and suction caisson foundations for offshore wind turbines. Comput Geotech 2021;134. http://dx.doi.org/10.1016/j.compgeo.2021.104107.
[26] Álamo GM, Padrón LA, Aznárez JJ, Maeso O. Numerical model for the dynamic and seismic analysis of pile-supported structures with a meshless integral representation of the layered soil. Bull Earthq Eng 2022;20(7):3215–38. http://dx.doi.org/10.1007/s10518-021-01287-7.
[27] Rovithis EN, Parashakis H, Mylonakis GE. 1D harmonic response of layered inhomogeneous soil: Analytical investigation. Soil Dyn Earthq Eng 2011;31(7):879–90. http://dx.doi.org/10.1016/j.soildyn.2011.01.007.
[28] Buckingham E. On physically similar systems; Illustrations of the use of dimensional equations. Phys Rev 1914;4:345–76. http://dx.doi.org/10.1103/PhysRev.4.345.
[29] Karatzia X, Mylonakis G. Discussion of "kinematic bending of fixed-head piles in nonhomogeneous soil" by raffaele di laora and emmanouil Rovithis. J Geotech Geoenviron Eng 2016;142(2):07015042. http://dx.doi.org/10.1061/(ASCE)GT.1943-5606.0001450.
[30] Álamo GM, Martínez-Castro AE, Padrón LA, Aznárez JJ, Gallego R, Maeso O. A proposal for normalized impedance functions of inclined piles in nonhomegenous media. Procedia Eng 2017;199:86–91. http://dx.doi.org/10.1016/j.proeng.2017.09.160.
[31] Miura K, Kaynia AM, Masuda K, Kitamura E, Seto Y. Dynamic behaviour of pile foundations in homogeneous and non-homogeneous media. Earthq Eng Struct Dynam 1994;23(2):183–92. http://dx.doi.org/10.1002/eqe.4290230206.